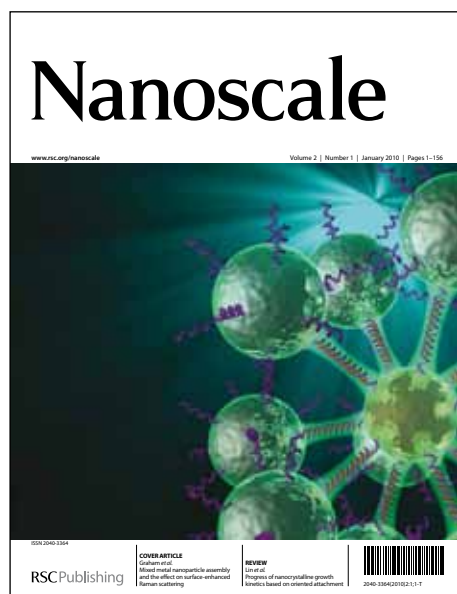


Nanoscale

Accepted Manuscript



This is an *Accepted Manuscript*, which has been through the RSC Publishing peer review process and has been accepted for publication.

Accepted Manuscripts are published online shortly after acceptance, which is prior to technical editing, formatting and proof reading. This free service from RSC Publishing allows authors to make their results available to the community, in citable form, before publication of the edited article. This *Accepted Manuscript* will be replaced by the edited and formatted *Advance Article* as soon as this is available.

To cite this manuscript please use its permanent Digital Object Identifier (DOI®), which is identical for all formats of publication.

More information about *Accepted Manuscripts* can be found in the [Information for Authors](#).

Please note that technical editing may introduce minor changes to the text and/or graphics contained in the manuscript submitted by the author(s) which may alter content, and that the standard [Terms & Conditions](#) and the [ethical guidelines](#) that apply to the journal are still applicable. In no event shall the RSC be held responsible for any errors or omissions in these *Accepted Manuscript* manuscripts or any consequences arising from the use of any information contained in them.

Cite this: DOI: 10.1039/c0xx00000x

www.rsc.org/xxxxxx

ARTICLE TYPE

Hierarchical Foam of Exposed Ultrathin Nickel Nanosheets Supported on Chainlike Ni-Nanowires and the Derivative Chalcogenide for Enhanced Pseudocapacitance

Wei Ni,^{* a,b} Bin Wang,^{a,b} Jianli Cheng,^{a,b} Xiaodong Li,^{a,b} Qun Guan,^{a,b} Guifang Gu^{a,b} and Ling Huang^{a,b}⁵ Received (in XXX, XXX) Xth XXXXXXXXX 20XX, Accepted Xth XXXXXXXXX 20XX

DOI: 10.1039/b000000x

Foamlike nickel hierarchical structures of ultrathin nanosheets supported on thin wires composed of nanoparticles are prepared by a facile one-pot synthesis via controlled nucleation and growth process. By further sulfidation, the sulfide derivative of loose porous fibrous structure shows a high electrochemical capacity for potential pseudocapacitor application.

Nanomaterials have received considerable attention and have shown significant advantages in the cutting-edge applications including catalysis and energy conversion and storage, due to their enhanced surface area and specific activity.^[1] Some two-dimensional (2D) nanosheet-like structures, such as graphene-based nanoassemblies, metal oxide or silicate lamellae, have been reported as new kinds of higher-specific-energy materials.^[2] These exotic 2D systems, which possess nanoscale dimensions only in thickness and have infinite length in the plane, are emerging as important new materials and recently intensively researched due to their unique properties.^[3] However, the 2D nanostructures, especially the ultrathin lamellae of transition or noble metals, have not yet been extensively exploited. There is limited literature available which shows that only a few kinds of elements have been successfully developed.^[2f, 4] Metallic 2D materials are rare and often difficult for direct fabrication by a wet chemical route, partly due to their higher surface energy. Though the high-temperature thermochemical reduction method was able to grow some metallic nanoplates or platelets,^[4a,b] a kind of relatively low-temperature solvent route is still challenging.

For the energy storage, batteries and capacitors are two commonly used, effective electrochemical devices. Compared to batteries, the supercapacitor including pseudocapacitor (i.e. redox supercapacitor) would offer a much higher power density and longer cycle life, making it a bright development perspective for e.g. electric vehicles (EVs) and heavy-duty applications for rapid and efficient delivery of electrical energy. The high power density of pseudocapacitor is primarily based on the high surface area and the rapid diffusion due to shortened path for the highly reversible Faradaic surface (redox) reactions.^[5a-c] Effects to develop more practical pseudocapacitive materials are now quite active.^[5a] At present the researches mostly focus on some promising active materials of, e.g., transition metal oxides,^[5d-f] although some materials such as nickel hydroxide (Ni(OH)₂) or

ruthenium dioxide (RuO₂) may possess higher capacitance or power density, yet they still find themselves limited in commercial applications due to relatively poor stability or high cost.^[6a-c] In recent years, the performances of metal hydroxides have been improved by a delicate hybridization with nanocarbon frameworks.^[7] Some researches on transition metal sulfides were also carried out and received high appraisals due to a comparable capacitance to that of hydroxides.^[8] In spite of not yet being so clear in the difference/relevance of the behaviors of sulfides in alkaline electrolytes with that of oxides or hydroxides, this kind of materials have show relatively higher stability than many hydroxides.^[9]

Taking transition metal nickel as a example, which can be fabricated into various nanostructures and morphologies by exquisite design and techniques,^[10] however, 2D nanosheets or nano-patches are still of rare breeds.^[11] As a continuation of our previous work,^[10e] we here reveal a route for the one-pot preparation of a novel surface topography of ultrathin layer structure, i.e. Ni nanosheets radiating from the homogenous Ni spine, by further regulation of the nucleation and growth process (Scheme 1), since it is well known that an important requirement in the fabrication of advanced inorganic materials and even some polymer materials is control over crystallization (i.e. crystal nucleation and growth), as well as Ostwald ripening or Kirkendall effect.^[12,13] The scanning electron microscopy (SEM, **Figure 1**) indicates that Ni nanoscale layers patch into thin wires, which further assembly into an intertwined structure and form a loose sponge-like morphology. The radiated nanosheets show a mean thickness of ~15 nm, which is comparable to that of previously reported value of *ca.* 10 nm of triangular and hexagonal single crystalline nanosheets,^[11b] ensuring more surface active sites exposed to the external environment. The X-ray diffraction (XRD) analysis confirms the face-centered cubic (fcc) phase structure of the as-synthesized samples with three typical characteristic peaks indexed as (111), (200), and (220) planes via reference to the Joint Commission on Powder Diffraction Standards database (JCPDS card no. 04-0850).^[10c] Through the transmission electron microscopy (TEM) it can be further found that the radiately grown nanosheets are actually composed of a geometrical axis (or spine) of chainlike polycrystalline thin wires, which may be nicknamed as 'Ni nanosheets intergrowth on homogeneous necklace-like backbones' or 'angry mini-snakes', and the

ultrathin metal Ni layer exhibits a very low contrast ratio to the visible amorphous carbon film on the TEM grid (**Figure 2**). With an altered nucleation process, the polyhedral crystals of the backbone of Ni thin wires were imperfectly developed, and left a graphene-like wrinkled lamellar or honeycomb-like microstructure (Figure S1 in ESI†), probably due to the competing reaction pathways for nanosheets and nanoparticles.

And this kind of metal nickel nanosheets undergoes a morphology and composition evolution via an air annealing. For instance, it may emerge with a minor NiO phase but with almost no morphology alteration; with higher annealing temperature, the metal Ni nanosheets become pierced by Kirkendall effect,^[13d] where the interface diffusion rate of oxygen and nickel atoms differ; at an even higher temperature, the nanosheets degrade dramatically into crystal whiskers and the backbone is simultaneously partially hollowed out and ends up with a pure NiO crystalline phase, proved by the related XRD spectra (**Figure 3**, and Figure S2 in ESI†). The conversion of such nanosheets by Kirkendall effect is somewhat distinguished from that of nanoparticles, i.e., resulting in a porous nanosheet-like structure rather than a hollow nanostructure.^[13c,d] The controllable oxidation may have conferred the pristine metal nanofoams with other properties or applications,^[14] such as catalysis for easier magnetic separation and recycling.

The novel hierarchically structured metal foam with more exposed surface, recently reported with another advantage for surface metallic layer^[15a], may provide a solid foundation for its superior performances and further applications.^[16] We here test the electrochemical properties as one of the potential applications.

An exquisite design and preparation of the nickel sulfide is derived from the above-mentioned nickel nanofoam. The general sulfidation process of inorganic materials uses sulfide precursors or hydrogen sulfide (H₂S) gas,^[4a, 17] however, the former will mainly be applicable in the initial stage of the product formation, and the latter is prone to a biological damage or environmental pollution. Here we have successfully tried an alternative solution by a high-pressure sulfur vapor to react with the as-prepared metal Ni nanosponge.^[18] The reaction takes place in a steel kettle sealed with Al-foil under 200–400 °C, and the sulfidation process can be accomplished in a short time such as 2 h with a recyclable deposited sulfur inside. The as-prepared black sponge at 300 °C for 2 h is determined to be nickel disulfide (NiS₂) by energy dispersive X-ray spectrum (EDS) and XRD analysis, and the crystal lattice is well consistent with the standard spectrum (JCPDS file no. 89-3058, 11-0099; see **Figure 4**), where the sharp peaks reveal a fine crystal structure and a cubic phase.^[15]

The macromorphology of the Ni nanosponge is well retained in the reaction process with sulfur vapor except for an increase in weight. From SEM observation it can be found that the Ni nanosheets on the thin-wire spine after sulfidation transformed into a polycrystalline layer of assembled polyhedral subsystems of NiS₂, along with some morphological degradation. The surface of the spine also appears some polyhedral polycrystalline structure, while the interior of the spine presents a porous structure (**Figure 5**), which can be mainly attributed to the above-mentioned Kirkendall effect as well. In the time-dependent sulfidation of Ni-nanofoam, sulfur vapor reacts readily with nickel nanocrystals at the boundaries, the predominant outward

diffusion of nickel through the sulfide shell, in addition to the inward transport of sulfur, results in supersaturation of vacancies, and leads to the formation of hollow or porous NiS_x nanostructures.^[13b,c,e] TEM observation validates the inward loose structure of the sulfide wires, and the selected area electron diffraction (SAED) verifies their polycrystal structure (elemental analysis by energy dispersive X-ray spectrum, EDS, see Figure S3 in ESI†). With the increase of sulfidation temperature e.g. up to 400 °C, a more obvious degradation of the thin layer structure emerges, and the whole thin wire eventually evolved into a polycrystalline, polyhedral assembled structure without nanosheets on the surface. Furthermore, the as-prepared NiS₂ can also be developed into different sulfides, oxides, or chalcogenides by controlling the pyrolysis environment and temperature (Figure S4 in ESI†).^[16]

The as-prepared sponge-like NiS₂ materials are composed of loose thin wires with nanocrystalline substructure, and hence would offer larger exposed surface and enhanced surface activity. As for the electrochemical activity in pseudocapacitor, the measurements are performed in a 2 M potassium hydroxide aqueous solution. NiS₂ active materials are loaded on a piece of commercial nickel foam (as current collector), which serves as working electrode, with platinum plate as counter electrode, and calomel electrode as reference. Cyclic voltammetry (CV) scanning shows that the oxidation/reduction peaks are at *ca.* 0.32 V and 0.16 V (with scanning rate of 1 mV s⁻¹), respectively; with an increasing rate of scanning, redox peaks move towards both ends separately (**Figure 6 a**).

In a constant current charge/discharge mode, as shown in Figure 6 b and Figure S5, it reveals an oxidation plateau at ~0.3 V, and reduction plateau ~0.2 V (with saturated calomel electrode, SCE, as reference), which is based on the valence conversion of Ni element during the redox reaction, with a probable formula as follows,



however there are also some reports arguing that the sulfides will eventually be transformed into hydroxides,^[19] which shows the complexity of reaction mechanism for sulfides as active electrode materials of pseudocapacitors. The peak area of oxidation and reduction shows a basic symmetry plus a sharp decline feature in each electrochemical discharge cycle beyond the reduction plateau, i.e. lower than 0.2 V. The calculation of the discharge capacity via the constant current mode, shows that the values of 1788, 1685, 1545, 1223, and 750 F g⁻¹, can be obtained at various current densities of 0.3, 1, 3, 10, and 30 A g⁻¹, respectively (Figure 6 c), according to an equation for specific capacitance as follows,

$$C_m = I \times \Delta t / (\Delta V \times m) \quad (2)$$

where C_m (F g⁻¹) indicates the specific capacitance, I (A) and Δt (s) are the discharge current and time, respectively, ΔV (V) is the potential change during discharge, and m (g) is the mass of active material in the electrode.

Figure 6 d shows the cycling performance of the as-prepared electrode materials. A range of specific capacity from *ca.* 1400 to 1000 F g⁻¹ can be delivered with a retention ratio of 78% after 1000 cycles, indicating its high capacitance and the cycling stability needs improvement via better adhesion to the current collector. The obtained capacity is even higher than that of the

general transition metal oxides, which can be probably attributed to its specific structure with higher exposed surface area and affinity for electrolyte solution, i.e. the hierarchical porous structure facilitates the electrolyte penetration and shortens the diffusion path of OH⁻.^[20] But the sulfides themselves may also gradually react with the aqueous alkaline solution by extension of time, which could lead to a reduction in adhesion to the current collector, electric conduction and capacity thereof. And a conductive carbon coating or composite may contribute to the further improvement of the performances.^[21]

In summary, here we have first exploited a novel one-pot approach for the large-scale, wet-chemical synthesis of hierarchical sponge-like metal nickel nanomaterials comprised of nanosheets-decorated thin wires. Furthermore, by an environment-friendly sulfur vapor post-treatment, the nickel sulfide derivatives can be obtained. The highly porous sulfide thin-wire material shows an extremely high capacitance and relatively good cycle performance, indicating its potential application in pseudocapacitors. This study may provide beneficial reference for the fabrication of other transition metal sulfides as supercapacitor electrode materials.

Experimental Section

For a typical synthesis of Ni foam of nanosheets-wrapped thin wires, into a 500-mL single-necked flask was added a nickel acetate/glycerol solution with mass ratio of 5 g vs. 250 g (Ni(Ac)₂·4H₂O, Aldrich; glycerol: Alfa Aesar) and followed by controlled refluxing at a tailor-made heating jacket of ca. 380 °C for ca. 40 min in atmospheric pressure with no magnetic stirring, the crystalline growth procedure was controlled at around 10 min or over, i.e. the period from initially turning black to the flocculent mass formation, by a controlled heat absorption power. A black and magnetic sponge would float on the liquid surface, it was then collected after cooling to room temperature, rinsed by deionized water with the assistance of a magnet, and dried at 60 °C overnight for further use. The sulfidation of as-synthesized Ni sponge was performed, by a high-pressure vapor-phase infusion/reaction method, in a self-made Al-foil-sealed steel autoclave with separately placed built-in container at 200–400 °C for 2–6 h (For further details see Figure S6 in ESI†).

The morphology and internal structure of materials were characterized by the field emission scanning electron microscopy (FESEM, JEOL JSM-6700F, 5 kV) and transmission electron microscopy (TEM, JEOL JEM-2010, 200 kV). Powder X-ray diffraction (XRD, Bruker D2 PHASER; Cu K α radiation, λ = 1.5406 Å) was used to identify the crystalline structure and composition of the materials. Energy dispersive X-ray spectroscopy (EDS) was performed on a SEM–X-ray microanalysis spectrometer (JEOL JED-2300) at an accelerating voltage of 15 kV. Thermogravimetric analysis (TGA, PerkinElmer Diamond TG/DTA) was carried out under a N₂/air flow of 200 mL min⁻¹ with a temperature ramp of 20 °C min⁻¹.

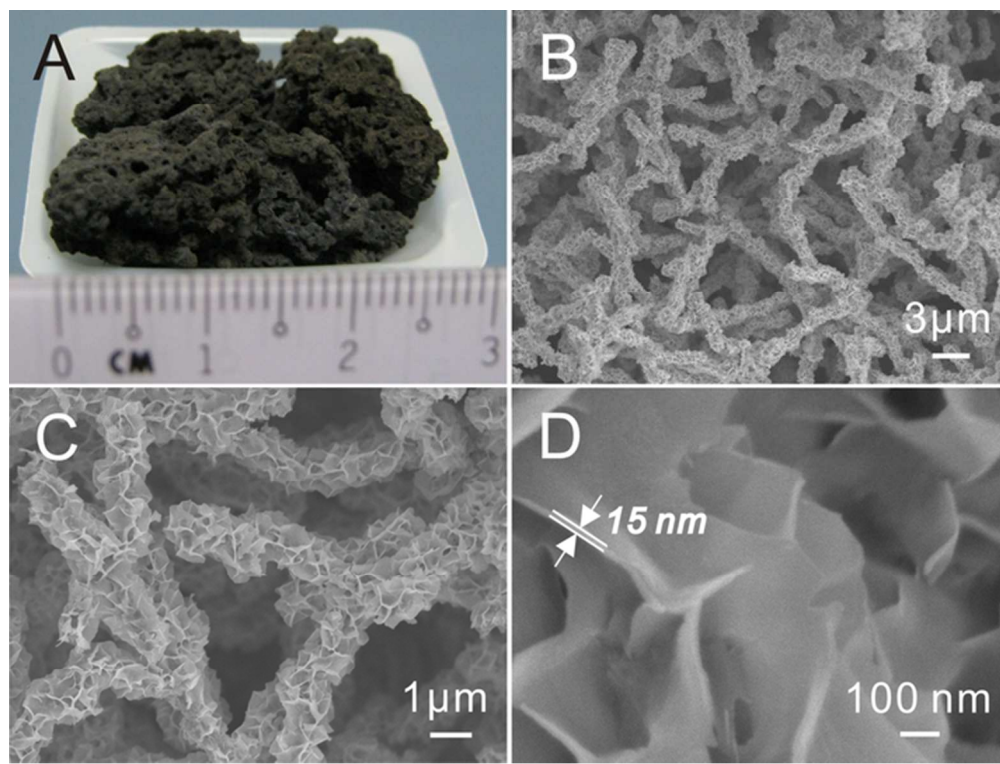
The slurry was prepared by mixing 80 wt% of the nickel sulfide, 10 wt% of Super P carbon black (Alfa Aesar) and 10 wt% of PVDF in NMP solution (Aldrich) as binder, and then coated on a commercial Ni-foam with active material content of ca. 3 mg cm⁻². Cyclic voltammetry (CV) studies were performed on a CHI 660 electrochemical workstation (CH Instruments).

Acknowledgement. The authors are grateful to Prof. Xiong Wen (David) Lou for allowing the use of synthesis and battery testing facilities in his laboratory, and to Prof. Rong Xu for her general support.

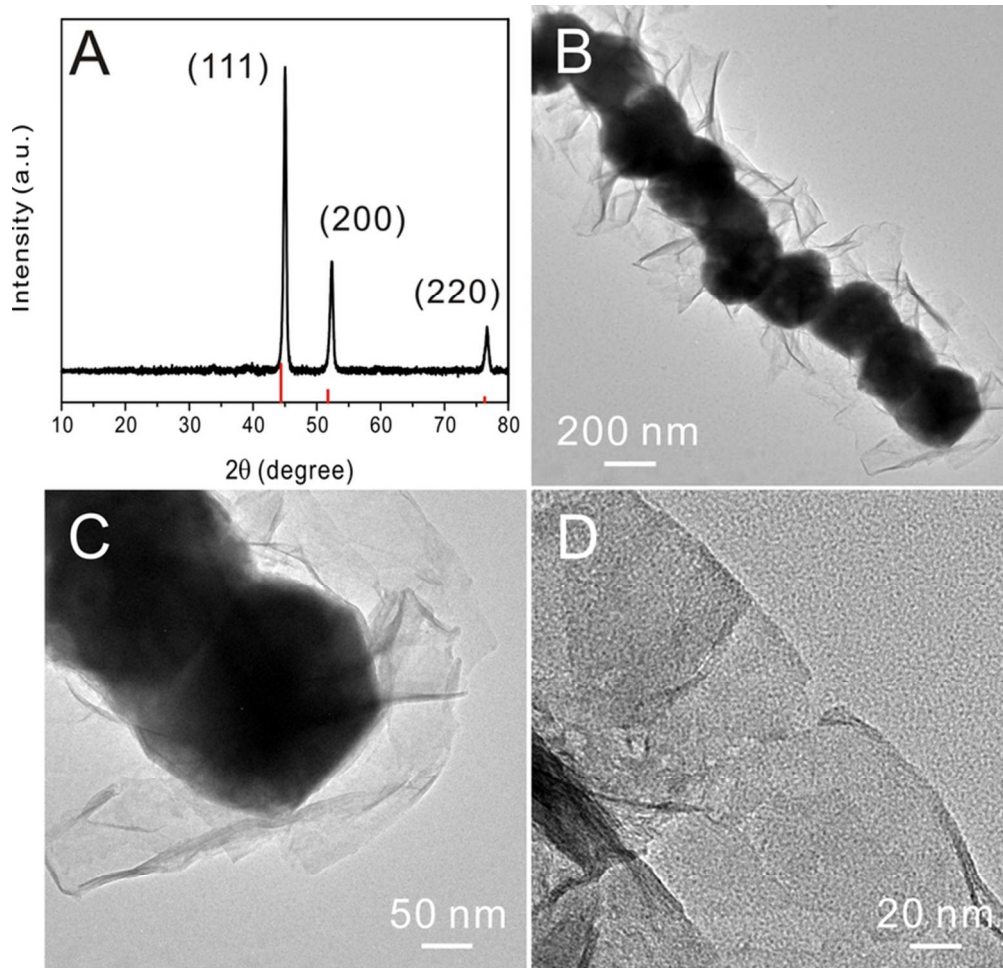
Notes and references

- ^a Institute of Chemical Materials, China Academy of Engineering Physics (CAEP), Mianyang 621900, China. Fax: +86 816-2544426; E-mail: niwei@iccas.ac.cn
- ^b Sichuan Research Center of New Materials, Mianyang 621000, China
- † Electronic Supplementary Information (ESI) available: SEM images, XRD patterns, EDS spectrum and TGA curves, and the charge/discharge profiles of Ni or NiS₂ materials, and the sketch of a tailor-made high-pressure sulfidation autoclave. See DOI: 10.1039/b000000x/
- a) A. S. Arico, P. Bruce, B. Scrosati, J.-M. Tarascon, W. van Schalkwijk, *Nat. Mater.* **2005**, *4*, 366-377; b) B. Dunn, H. Kamath, J.-M. Tarascon, *Science* **2011**, *334*, 928-935; c) X. W. Lou, L. A. Archer, Z. Yang, *Adv. Mater.* **2008**, *20*, 3987-4019; d) Y.-G. Guo, J.-S. Hu, L.-J. Wan, *Adv. Mater.* **2008**, *20*, 2878-2887.
 - a) Y. Sun, Q. Wu, G. Shi, *Energy Environ. Sci.* **2011**, *4*, 1113-1132; b) P. V. Kamat, *J. Phys. Chem. Lett.* **2011**, *2*, 242-251; c) M. D. Stoller, S. Park, Y. Zhu, J. An, R. S. Ruoff, *Nano Lett.* **2008**, *8*, 3498-3502; d) J. S. Chen, X. W. Lou, *Mater. Today* **2012**, *15*, 246-254; e) K. Varoon, X. Zhang, B. Elyassi, D. D. Brewer, M. Gettel, S. Kumar, J. A. Lee, S. Maheshwari, A. Mittal, C.-Y. Sung, M. Cococcioni, L. F. Francis, A. V. McCormick, K. A. Mkhoyan, M. Tsapatsis, *Science* **2011**, *334*, 72-75; f) W.-F. Chen, K. Sasaki, C. Ma, A. I. Frenkel, N. Marinkovic, J. T. Muckerman, Y. Zhu, R. R. Adzic, *Angew. Chem. Int. Ed.* **2012**, *51*, 6131-6135.
 - a) M. Osada, T. Sasaki, *J. Mater. Chem.* **2009**, *19*, 2503-2511; b) J. N. Coleman, M. Lotya, A. O'Neill, S. D. Bergin, P. J. King, U. Khan, K. Young, A. Gaucher, S. De, R. J. Smith, I. V. Shvets, S. K. Arora, G. Stanton, H.-Y. Kim, K. Lee, G. T. Kim, G. S. Duesberg, T. Hallam, J. J. Boland, J. J. Wang, J. F. Donegan, J. C. Grunlan, G. Moriarty, A. Shmeliov, R. J. Nicholls, J. M. Perkins, E. M. Grievson, K. Theuwissen, D. W. McComb, P. D. Nellist, V. Nicolosi, *Science* **2011**, *331*, 568-571; c) C. Zhong, J. Wang, Z. Chen, H. Liu, *J. Phys. Chem. C* **2011**, *115*, 25115-25120.
 - a) Y.-C. Zhu, Y. Bando, *Chem. Phys. Lett.* **2003**, *372*, 640-644; b) J. Zhao, C. Ye, X. Fang, P. Yan, L. Zhang, *Mater. Chem. Phys.* **2006**, *99*, 206-209; c) Z. Li, Z. Liu, J. Zhang, B. Han, J. Du, Y. Gao, T. Jiang, *J. Phys. Chem. B* **2005**, *109*, 14445-14448.
 - a) J. R. Miller, P. Simon, *Science* **2008**, *321*, 651-652; b) A. G. Pandolfo, A. F. Hollenkamp, *J. Power Sources* **2006**, *157*, 11-27; c) D. Wei, M. R. J. Scherer, C. Bower, P. Andrew, T. Ryhänen, U. Steiner, *Nano Lett.* **2012**, *12*, 1857-1862; d) X. Lang, A. Hirata, T. Fujita, M. Chen, *Nat. Nanotechnol.* **2011**, *6*, 232-236; e) P. Simon, Y. Gogotsi, *Nat. Mater.* **2008**, *7*, 845-854; f) G. Wang, L. Zhang, J. Zhang, *Chem. Soc. Rev.* **2012**, *41*, 797-828.
 - a) A. Burke, *J. Power Sources* **2000**, *91*, 37-50; b) G. Hu, C. Li, H. Gong, *J. Power Sources* **2010**, *195*, 6977-6981; c) G.-W. Yang, C.-L. Xu, H.-L. Li, *Chem. Commun.* **2008**, 6537-6539.
 - a) Z. Tang, C.-H. Tang, H. Gong, *Adv. Funct. Mater.* **2012**, *22*, 1272-1278; b) H. Wang, H. S. Casalongue, Y. Liang, H. Dai, *J. Am. Chem. Soc.* **2010**, *132*, 7472-7477.
 - a) B. Zhang, X. Ye, W. Dai, W. Hou, Y. Xie, *Chem. Eur. J.* **2006**, *12*, 2337-2342; b) T. Zhu, Z. Wang, S. Ding, J. S. Chen, X. W. Lou, *RSC Adv.* **2011**, *1*, 397-400; c) S.-J. Bao, C. M. Li, C.-X. Guo, Y. Qiao, *J. Power Sources* **2008**, *180*, 676-681; d) J.-Y. Lin, S.-W. Chou, *RSC Adv.* **2013**, *3*, 2043-2048.
 - S. Lichušina, A. Chodosovskaja, K. Leinartas, A. Selskis, E. Juzeliūnas, *J. Solid State Electrochem.* **2010**, *14*, 1577-1584.
 - a) M. Han, Q. Liu, J. He, Y. Song, Z. Xu, J. M. Zhu, *Adv. Mater.* **2007**, *19*, 1096-1100; b) C. Gong, L. Yu, Y. Duan, J. Tian, Z. Wu, Z. Zhang, *Eur. J. Inorg. Chem.* **2008**, 2884-2891; c) L.-P. Zhu, G.-H. Liao, W.-D. Zhang, Y. Yang, L.-L. Wang, H.-Y. Xie, *Eur. J. Inorg. Chem.* **2010**, 2010, 1283-1288; d) Q. Liu, H. Liu, M. Han, J. Zhu, Y. Liang, Z. Xu, Y. Song, *Adv. Mater.* **2005**, *17*, 1995-1999; e)

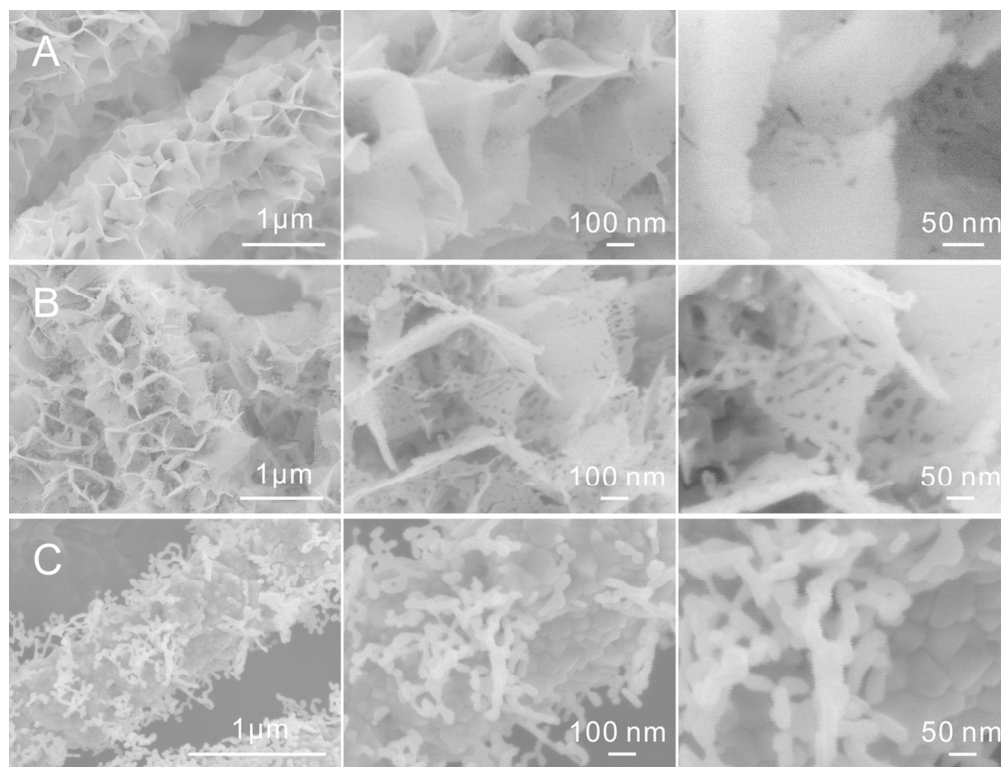
- W. Ni, H. B. Wu, B. Wang, R. Xu, X. W. Lou, *Small* **2012**, *8*, 3432-3437.
- 11 a) Y. Leng, Y. Wang, X. Li, T. Liu, S. Takahashi, *Nanotechnology* **2006**, *17*, 4834; b) Y. Leng, Y. Zhang, T. Liu, M. Suzuki, X. Li, *Nanotechnology* **2006**, *17*, 1797.
- 5 12 a) J. Aizenberg, A. J. Black, G. M. Whitesides, *Nature* **1999**, *398*, 495-498; b) B. Wiley, Y. Sun, Y. Xia, *Acc. Chem. Res.* **2007**, *40*, 1067-1076; c) Y. Xia, Y. Xiong, B. Lim, S. E. Skrabalak, *Angew. Chem. Int. Edit.* **2009**, *48*, 60-103; d) Y. Su, G. Liu, B. Xie, D. Fu, D. Wang, *Acc. Chem. Res.* DOI: 10.1021/ar400116c.
- 10 13 a) H. C. Zeng, *Curr. Nanosci.* **2007**, *3*, 177-181; b) H. J. Fan, U. Gösele, M. Zacharias, *Small* **2007**, *3*, 1660-1671; c) Y. Yin, R. M. Rioux, C. K. Erdonmez, S. Hughes, G. A. Somorjai, A. P. Alivisatos, *Science* **2004**, *304*, 711-714; d) J. G. Railsback, A. C. Johnston-Peck, J. Wang, J. B. Tracy, *ACS nano* **2010**, *4*, 1913-1920; e) Y. Yin, C. K. Erdonmez, A. Cabot, S. Hughes, A. P. Alivisatos, *Adv. Funct. Mater.* **2006**, *16*, 1389-1399.
- 14 S. Han, H.-Y. Chen, C.-C. Chen, T.-N. Yuan, H. C. Shih, *Mater. Lett.* **2007**, *61*, 1105-1108.
- 20 15 a) K. D. M. Rao, T. Bhuvana, B. Radha, N. Kurra, N. S. Vidhyadhiraja, G. U. Kulkarni, *J. Phys. Chem. C* **2011**, *115*, 10462-10467; b) X. Qian, Y. Li, Y. Xie, Y. Qian, *Mater. Chem. Phys.* **2000**, *66*, 97-99; c) P. R. Bonneau, R. K. Shiao, R. B. Kaner, *Inorg. Chem.* **1990**, *29*, 2511-2514; d) C. L. Stender, T. W. Odom, *J. Mater. Chem.* **2007**, *17*, 1866-1869; e) S.-H. Yu, M. Yoshimura, *Adv. Funct. Mater.* **2002**, *12*, 277-285.
- 25 16 F. A. Harraz, R. M. Mohamed, A. Shawky, I. A. Ibrahim, *J. Alloys Compd.* **2010**, *508*, 133-140.
- 17 a) A. Ghezelbash, M. B. Sigman, B. A. Korgel, *Nano Lett.* **2004**, *4*, 537-542; b) Y. Hu, J. Chen, W. Chen, X. Lin, X. Li, *Adv. Mater.* **2003**, *15*, 726-729; c) C. L. Stender, T. W. Odom, *J. Mater. Chem.* **2007**, *17*, 1866-1869.
- 30 18 a) L. Zhang, J. C. Yu, M. Mo, L. Wu, Q. Li, K. W. Kwong, *J. Am. Chem. Soc.* **2004**, *126*, 8116-8117; b) S. Huang, X. Liu, Q. Li, M. Meng, T. Long, Z. Jiang, *Solid State Sci.* **2011**, *13*, 1375-1378.
- 35 19 L. Hou, C. Yuan, D. Li, L. Yang, L. Shen, F. Zhang, X. Zhang, *Electrochim. Acta* **2011**, *56*, 7454-7459.
- 20 a) M.-S. Wu, Y.-A. Huang, J.-J. Jow, W.-D. Yang, C.-Y. Hsieh, H.-M. Tsai, *Int. J. Hydrogen Energy* **2008**, *33*, 2921-2926; b) M.-S. Wu, M.-J. Wang, *Chem. Commun.* **2010**, *46*, 6968-6970.
- 40 21 T. Zhu, H. B. Wu, Y. Wang, R. Xu, X. W. Lou, *Adv. Energy Mater.* **2012**, *2*, 1497-1502.



60x45mm (300 x 300 DPI)



70x67mm (300 x 300 DPI)



114x86mm (300 x 300 DPI)

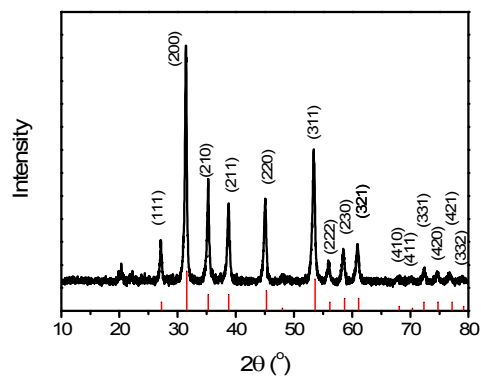
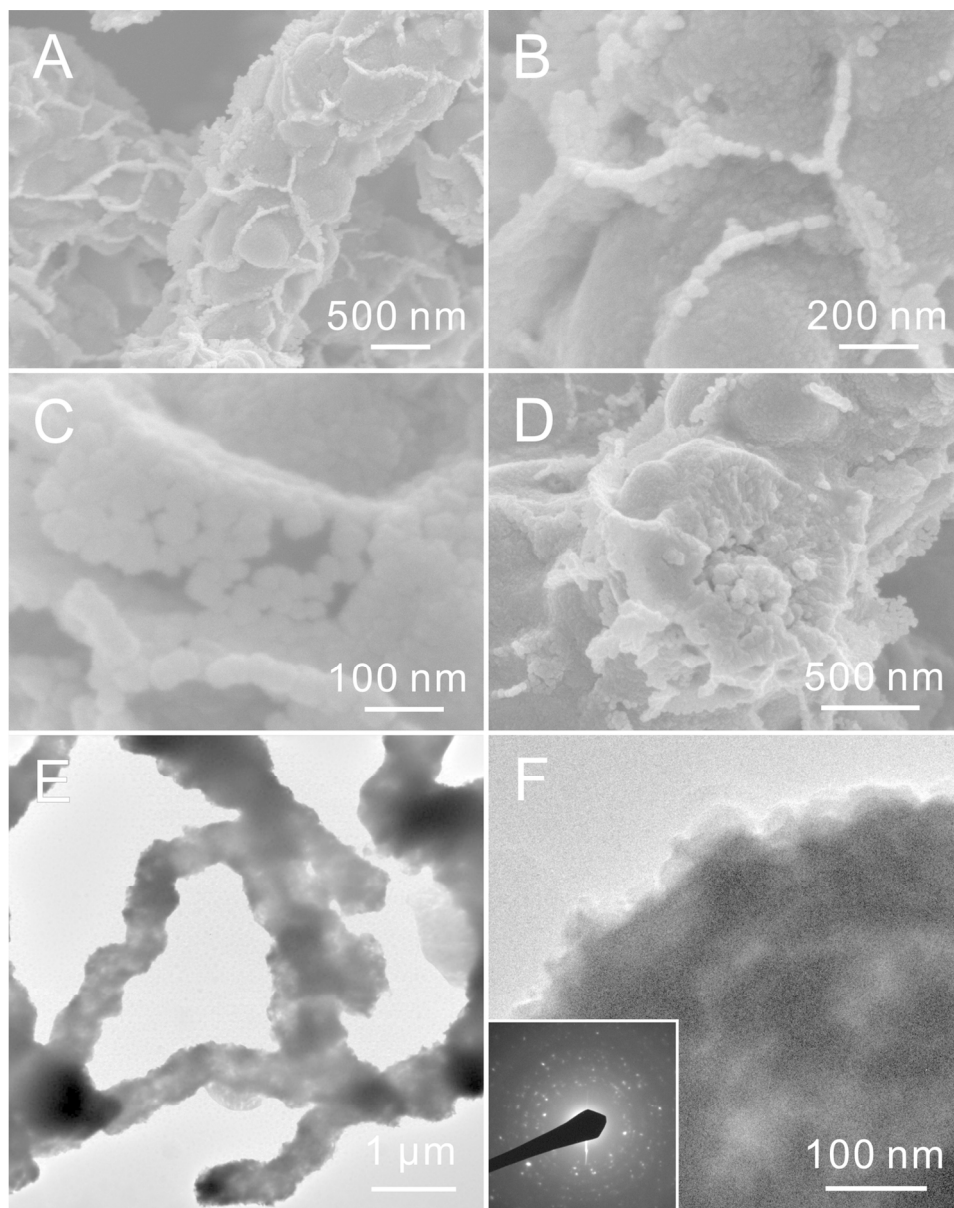
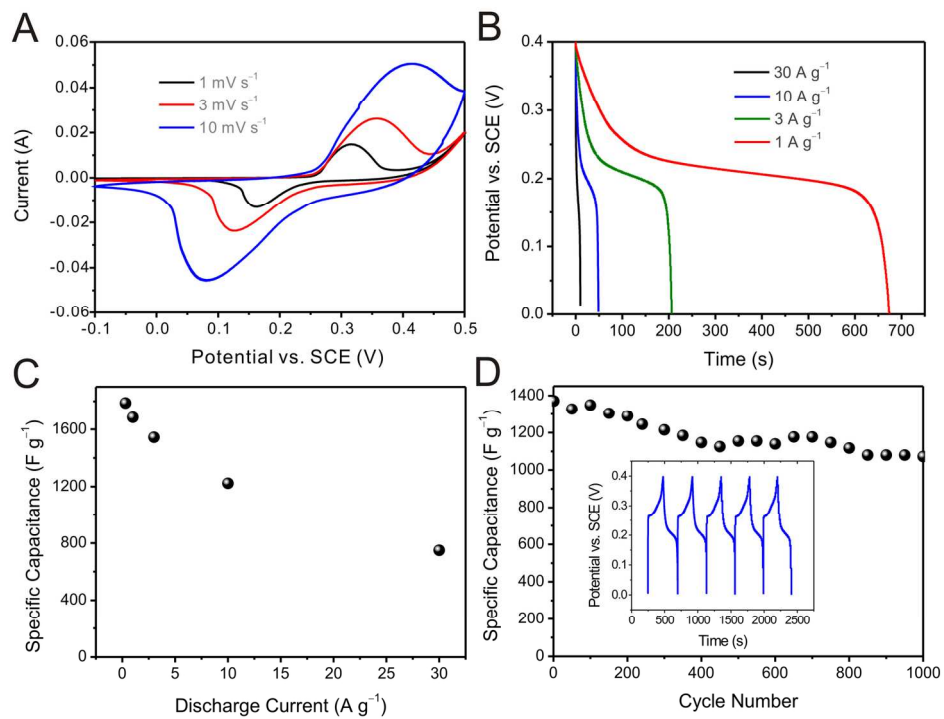


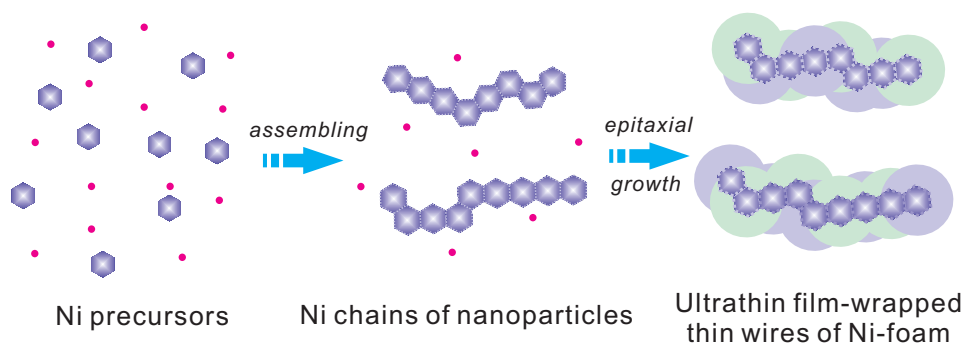
Fig. 4 XRD spectrum of the NiS₂ nanofoam by high-pressure sulfur-vapor-phase reaction at 300 °C for 2 h (NiS₂, JCPDS no. 89-3058, 11-0099).

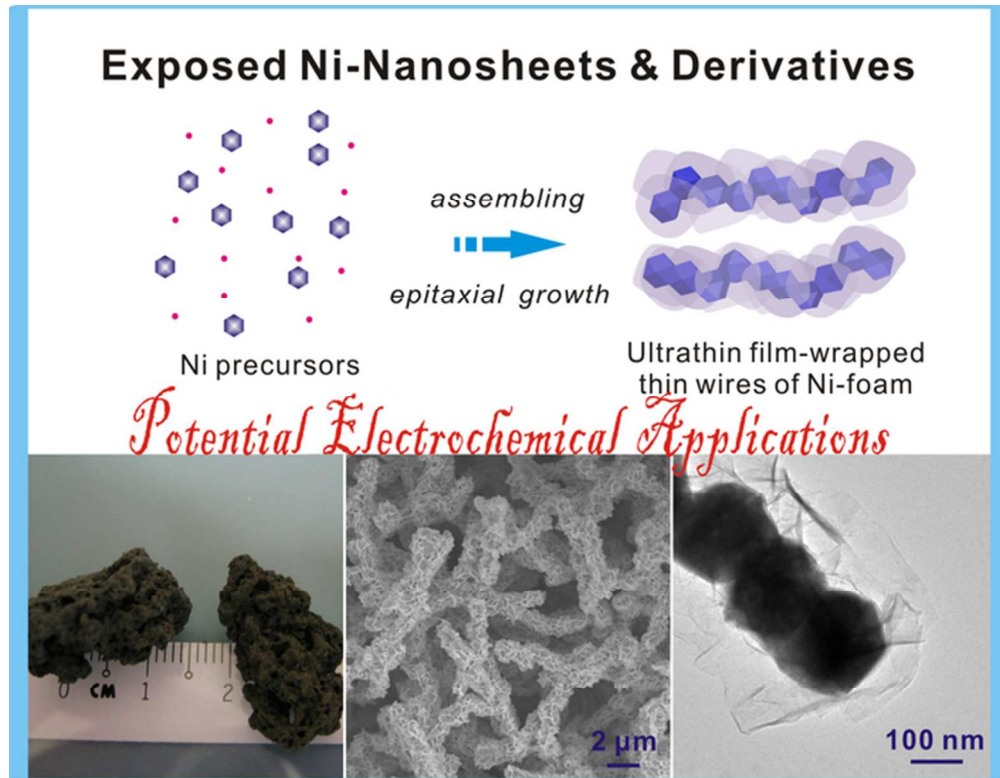


126x158mm (300 x 300 DPI)



153x111mm (300 x 300 DPI)





Hierarchical nickel of exposed ultrathin nanosheets on thin-wire backbones is controllably synthesized and NiS₂ derivative shows high capacity for pseudocapacitors.
59x46mm (300 x 300 DPI)